

## MICROVASCULAR PATTERNS OF THE HUMAN LARGE INTESTINE: MORPHOMETRIC STUDIES OF VASCULAR PARAMETERS IN CORROSION CASTS

E. Fait, W. Malkusch<sup>1</sup>, S.-H. Gnoth, Ch. Dimitropoulou,  
A. Gaumann<sup>2</sup>, C.J. Kirkpatrick<sup>2</sup>, Th. Junginger<sup>3</sup> and M.A. Konerding\*

Anatomisches Institut, Johannes Gutenberg-Universität Mainz, Becherweg 13, D-55099 Mainz; <sup>1</sup>Kontron Elektronik GmbH, Oskar-van-Miller Str. 1, D-85385 Eching b. München; <sup>2</sup>Pathologisches Institut and <sup>3</sup>Klinikum und Poliklinikum für Allgemein- und Abdominalchirurgie, Johannes Gutenberg-Universität Mainz, D-55101 Mainz

(Received for publication October 25, 1996 and in revised form March 14, 1997)

### Abstract

The microvascularization of 19 human colonic segments was studied quantitatively by means of scanning electron microscopy of microvascular corrosion casts. In total, four caecums, two ascending and four descending colons, six sigmoidal colons and four rectums were examined. In order to describe quantitatively the microvascular unit, three parameters were assessed: (1) intercapillary distances, (2) interbranching distances and (3) branching angles. All parameters were measured in stereo pairs of microvascular corrosion casts using an interactive image analyzing system. Examination of microvascular corrosion casts showed the mucosal capillary network arranged in a honeycomb pattern around the mucosal glands. This meshwork is supplied by arterioles and subepithelial capillaries and drained by venules which merge to submucosal veins. The average value for the intercapillary distances is  $107.2 \pm 27.6 \mu\text{m}$ , for the interbranching distances  $51.3 \pm 28.5 \mu\text{m}$  and for the branching angles  $87.4 \pm 29.2^\circ$ . Comparisons of the quantified parameters within a given segment as well as group comparisons of all segments did not reveal any significant inter-individual difference.

**Key Words:** Microvascularization, corrosion casting, scanning electron microscopy, microvascular unit, caecum, colon, rectum, morphometry.

\*Address for correspondence:

Moritz A. Konerding  
Anatomisches Institut, Makroskopischer Bereich  
Johannes Gutenberg-Universität Mainz  
Becherweg 13  
D-55099 Mainz, Germany  
Telephone number: 49-6131-392549  
Fax number: 49-6131-394710  
E-mail: konerdin@mzdmza.zdv.uni-mainz.de

### Introduction

Scanning electron microscopy (SEM) of microvascular corrosion casts is one of the most useful methods for obtaining insights into the microvascular patterns of circulatory pathways. The important advantage of this method is that the whole terminal blood stream from the arterial to the venous segment including the capillary bed can be clearly shown. Furthermore, the casting medium replicates numerous topographical details of the endothelial luminal surface, thus the direction of blood flow can be determined indirectly from the length-breadth relation of the nuclear impressions (Christofferson and Nilsson, 1990). For detailed reviews, see Lametschwandtner *et al.* (1980, 1984, 1990) and Konerding (1991).

However, most studies using this technique confine themselves to qualitative descriptions, although there is a strong need for reproducible quantitative data as recently postulated by Konerding *et al.* (1995). Scanning electron microscopy allows for three-dimensional representation and morphometry with little error. Malkusch *et al.* (1995) demonstrated a feasible approach in calculating a variety of vascular parameters based on 3D-stereo pairs of microvascular corrosion casts. The microvascular unit could be characterized by three parameters, the intercapillary as well as the interbranching distances and the branching angles.

The special biological, physiological and morphological properties of the colon have given rise to numerous microvascular investigations (e.g., Aharinejad *et al.*, 1991, 1992; Darien *et al.*, 1993; Skinner *et al.*, 1995). For example, the maintenance of electrolyte equilibrium is regulated both by kidney and colon; a further point of interest is the absorption of water. These resorptive processes strongly depend on the blood flow.

Until today, the microvascularity of the colon was studied qualitatively in humans (Skinner *et al.*, 1995), horse (Dart *et al.*, 1992; Darien *et al.*, 1993), guinea pig (Aharinejad *et al.*, 1991, 1992) or rat (Browning and Gannon, 1986; Skinner *et al.*, 1990).

From the oncological point of view, such data seem to be of importance, too, because of the high incidence of

**Table 1.** Numeric distribution of the investigated colonic segments.

Segment	Number of specimens
caecum	3
ascending colon	2
descending colon	4
sigmoidal colon	6
rectum	4

colonic carcinomas (Konerding *et al.*, 1995). Against this background, the aim of this study was to determine the human colonic microvascular pattern both qualitatively and quantitatively and to compare the microcirculatory units of the individual colon segments, in order to get quantitative data for further comparative studies of the microvascularisation, e.g., of tumors of the large intestine.

## Materials and Methods

### Specimens

A total of 19 colon specimens obtained in a seven month period from patients undergoing colonic resections was studied. In most cases, colonic resection was performed because of malignant tumors. The patient group was not selected; ten were males, nine females, with an average age of  $65 \pm 11$  years. For the distribution of the colonic segments, see Table 1. The studies were performed according to both legal and ethical regulations.

### Microvascular corrosion casting

The resected segments of the large intestine were transported in a closed container without any storage solution within 15-20 minutes after surgery to the Department of Anatomy. Between one and four olive tipped cannulas (Kratz, Dreieich, Germany) were inserted into the major mesenteric arterial vessels supplying the segment of the large intestine. Segments of the caecum and ascending colon were perfused through the ileocaecal artery or the caecal artery. For perfusion of descending colon, branches of the left colonic artery or sigmoidal artery were cannulated. Rectal segments were perfused through the sigmoidal or superior rectal artery.

Blood was washed out by infusion of body-warm (36-38°C) physiological saline (0.9% NaCl, pH 7.4, buffered with phosphate-buffered saline, PBS, 850 mosmol) added with 8000 U/L heparin (Liquemin N 25000, Hoffmann-La Roche, Grenzach-Wyhlen, Germany) with manually controlled pressure.

The cut edges of the specimens were clamped to

ensure circulation of the washout and fixation solution through the specimens. When the wash-out from the veins was clear (approximately 3-5 minutes after commencing the wash-out, 300-400 ml of heparinized saline), up to 100 ml of 2.5% bodywarm glutaraldehyde (pH = 7.40, 850 mosmol, buffered with PBS) as fixative (Bioproducts, Boehringer Ingelheim, Germany) was perfused for 1-2 minutes. A methacrylate based acrylic resin solution prepared by mixing 15 ml of Mercox CL-2B, 0.1 g of catalyst MA (Vilene Med. Co., Tokyo, Japan), and 5 ml of Methylmethacrylate monomers (Merck, Darmstadt, Germany) was used as casting medium in a 20 ml syringe. 80-120 ml of the casting medium were infused under manually controlled pressure via the olive tipped cannulas. A 3-way stopcock enabled an air-bubble-free change of the syringes during perfusion of the microvascular network.

The resin was allowed to polymerize in a water-bath at 36-38°C, for approximately 40 minutes. Following this, from each specimen three to four samples of 2 cm x 2 cm were taken out at a distance of at least 10 cm from the malignant tumor. Subsequently, the surgical specimen was fixed in 4% formalin and brought to the Department of Pathology for histopathological diagnosis. Extensive preceding experiments, which were carried out before this study on human surgical specimens, have shown that the casting procedure does not interfere with the histopathological diagnosis.

Sections of the specimens which were extremely rich in fat were immersed in a soap solution for 24 hours at a temperature of 37°C. Maceration was carried out in 7% potassium hydroxide (Fluka, Neu-Ulm, Germany) at 40°C for 2-4 days. The solution was changed every day. The corrosion casts were cleaned by washing with distilled water. All specimens were freeze dried (ALPHA II-12, Vakuumentchnik GmbH, Wertheim/Main, Germany), mounted onto specimen stubs (BAL-TEC AG, Walluf, Germany) with conductive silver paste (Plano, Marburg, Germany), and stabilised with conductive bridges according to Lametschwandtner *et al.* (1990). The specimens were coated with gold in an argon atmosphere with a thickness of 40-45 nm at an amperage of 30-35 nA (BAL-TEC AG). Examination of the microvascular corrosion casts was carried out with a Stereoscan Mk-250 scanning electron microscope (Cambridge, U.K.), using an acceleration voltage of 10 kV, magnifications between 80 and 500 fold, and a working distance of at least 10 mm. For morphometric analysis, of each specimen at least 20 stereo pairs were taken using a tilt angle difference of exactly 6°. The specimens were tilted on an eucentric specimen stage which was calibrated by means of a goniometer. Ilford FP4 films (36 mm; Ilford, U.K.) were used for photographic recording.

### Morphometry of microvasculature corrosion casts

The stereo pairs were scanned with a black/white-



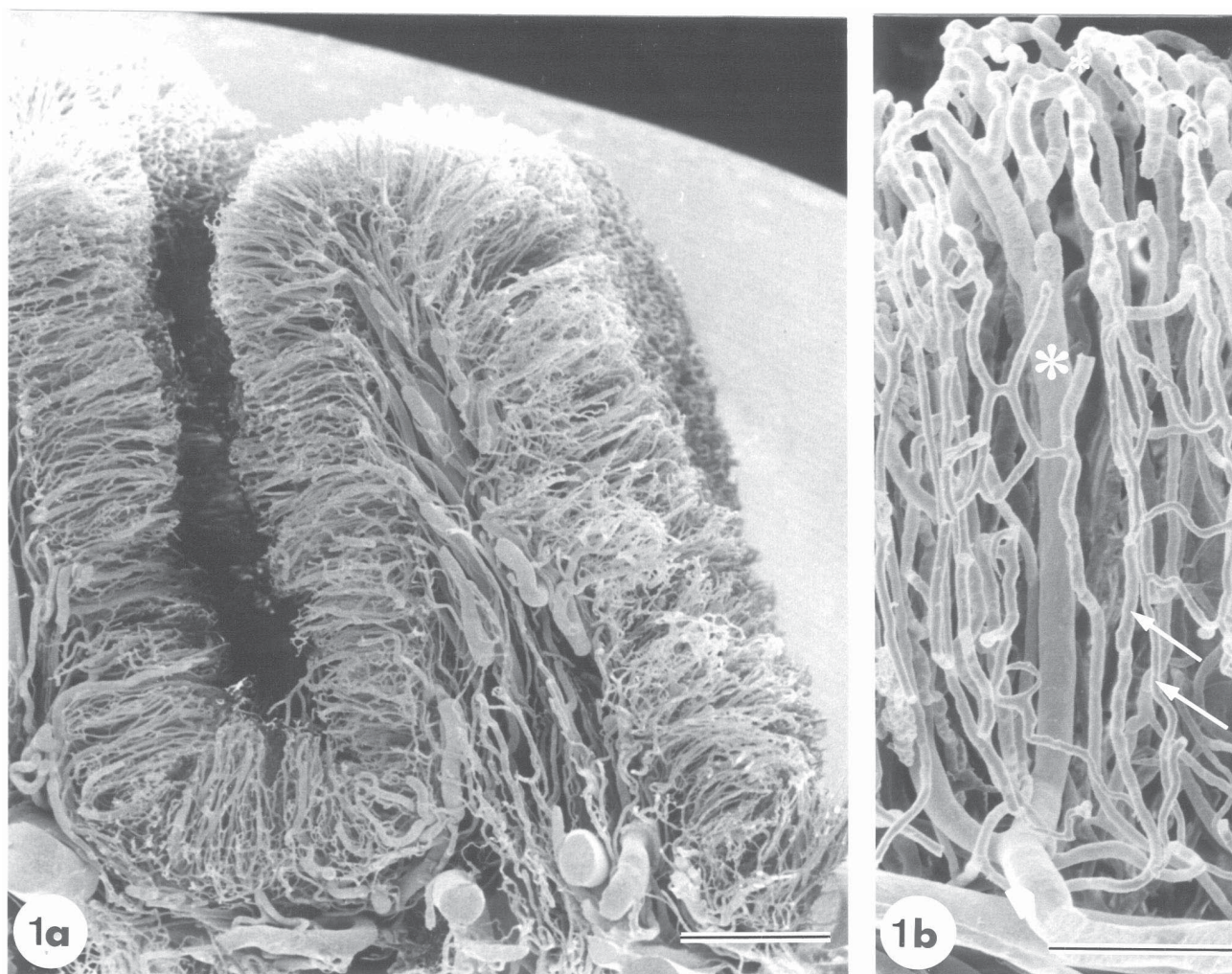


**Figure 1.** Scanning electron micrographs of a microvascular corrosion cast of the proximal human rectum (cross section) showing arteries and veins from the muscularis and microvessels of the mucosa and submucosa (**a** and **b**). The mucosal capillary network is supplied by arterioles (arrows), which divide into capillaries (small asterisk) at the level of the submucosa (**b**). Capillaries then form the honeycomb plexus and drain into venules (large asterisk) at the luminal surface of the mucosa, these venules then pass to submucosal veins (bold arrow). Bars = 1 mm (a) and 200  $\mu\text{m}$  (b).

video camera with a 2/3-CCD (charge couple device)-video camera (AVT-BC 1, AVT-Horn, Germany), digitised with a framegrabber board (Kontron Elektronik, Eching, Germany) with a depth of 8 bit and stored in a PC-based image processing system (KS 300, Kontron Elektronik). The images were stored in an img-format. Preceding the measurements, some image processing steps (filters), including the stretching of the grey value over the whole range of 256 grey levels, were performed to enhance the contrast as well as the brightness.

In order to calculate the 3D-coordinates of the microvascular corrosion casts, all points were alternately marked in both stereo images using the computer mouse.

The coordinates of the left stereo image were counted as x- and y-coordinates, whereas the values of the corresponding points in the right stereo pair were counted as x'- and y'-coordinates. All values were stored in a results table (Excel, Microsoft). To calculate true distances it is essential that the y- and the y'-coordinates coincide (Malkusch *et al.*, 1995). To perform quantitative evaluations from the corrosion casts, the z-coordinate (= object height, z) has to be calculated using the common mathematic parallax ( $P = P_x - P_x'$ ) and the known tilt angle  $\alpha$  (Boyde, 1973, 1974). For the mathematical basis of calculating true values of the interbranching distance, intercapillary distance and branching angle as well as for the error possibilities and

**Table 2.** Average values of the intercapillary distances, interbranching distances and branching angles of different segments of the large intestine expressed with deviation of the mean ( $m \pm SD$ ), plus the number of measurements.

		Segment of the large intestine			
		caecum	colon	sigmoidal colon	rectum
Intercapillary distance	mean ( $\mu\text{m}$ ) $\pm$ deviation	98.09 $\pm$ 22.8	102.0 $\pm$ 22.6	101.9 $\pm$ 23.9	107.8 $\pm$ 23.6
	minimum	49.7	51.4	41.7	52.2
	maximum	196.2	171.3	170.3	181.2
	number of measurements	315	306	264	203
Interbranching distance	mean ( $\mu\text{m}$ ) $\pm$ deviation	46.2 $\pm$ 27.8	50.5 $\pm$ 26.2	50.6 $\pm$ 26.5	56.1 $\pm$ 33.6
	minimum	10.6	8.2	9.02	11.7
	maximum	229.2	214.5	206.3	238.5
	number of measurements	457	1103	763	678
Branching angle	mean ( $^\circ$ ) $\pm$ deviation	86.8 $\pm$ 29.6	87.9 $\pm$ 26.6	87.8 $\pm$ 29.4	89.1 $\pm$ 27.5
	minimum	15.8	7.4	8.1	15.0
	maximum	150.2	167.9	167.7	145.9
	number of measurements	397	663	583	391

**Figure 2** (on the facing page). Scanning electron microscopic illustration of the typical honeycomb pattern of the vessels of a mucosal fold of the human colon (border between caecum and ascending colon). This homogeneous arrangement of the capillary plexus around the mucosal glands is found within all investigated segments (a). The higher magnification (b) of (a) reveals the detailed arrangement of microvessels around the mucosal glands (asterisk). This hexagonal capillary plexus is supplied by subepithelial arterioles (bold arrow) (b). The mucosal capillaries drain into venules (star). Note the numerous cross-connections (small arrows) of the capillaries.

In Figure 2b, in the upper right, point definition examples for the determination of the intercapillary distances are given. In the lower left, examples for the determination of the interbranching distances, and in the upper left, an example for the determination of the branching angles. The size of the points in these examples was increased for better visibility. The original point size was  $2 \times 2$  pixels. Bars = 1 mm (a) and  $100 \mu\text{m}$  (b).

calibration, see Malkusch *et al.* (1995). From the x-, y- and z-coordinate, all other true parameters can be calculated in the 3D-space. For each investigated parameter, at least 80 independent measurements per specimen were carried out.

The graphic demonstration and statistics were done using SigmaPlot and SigmaStat (Jandel Scientific Software, Erkrath, Germany). All groups were verified for normality before statistic calculation. The class distributions were tested for significance using the Chi-square test, whereas testing for significant differences in mean standard deviation was performed with the Mann-Whitney rank sum test. In all cases, the sensitivity was assessed by means of a power calculation, which revealed  $\delta$  values higher than 0.9 at the 5% level of confidence.

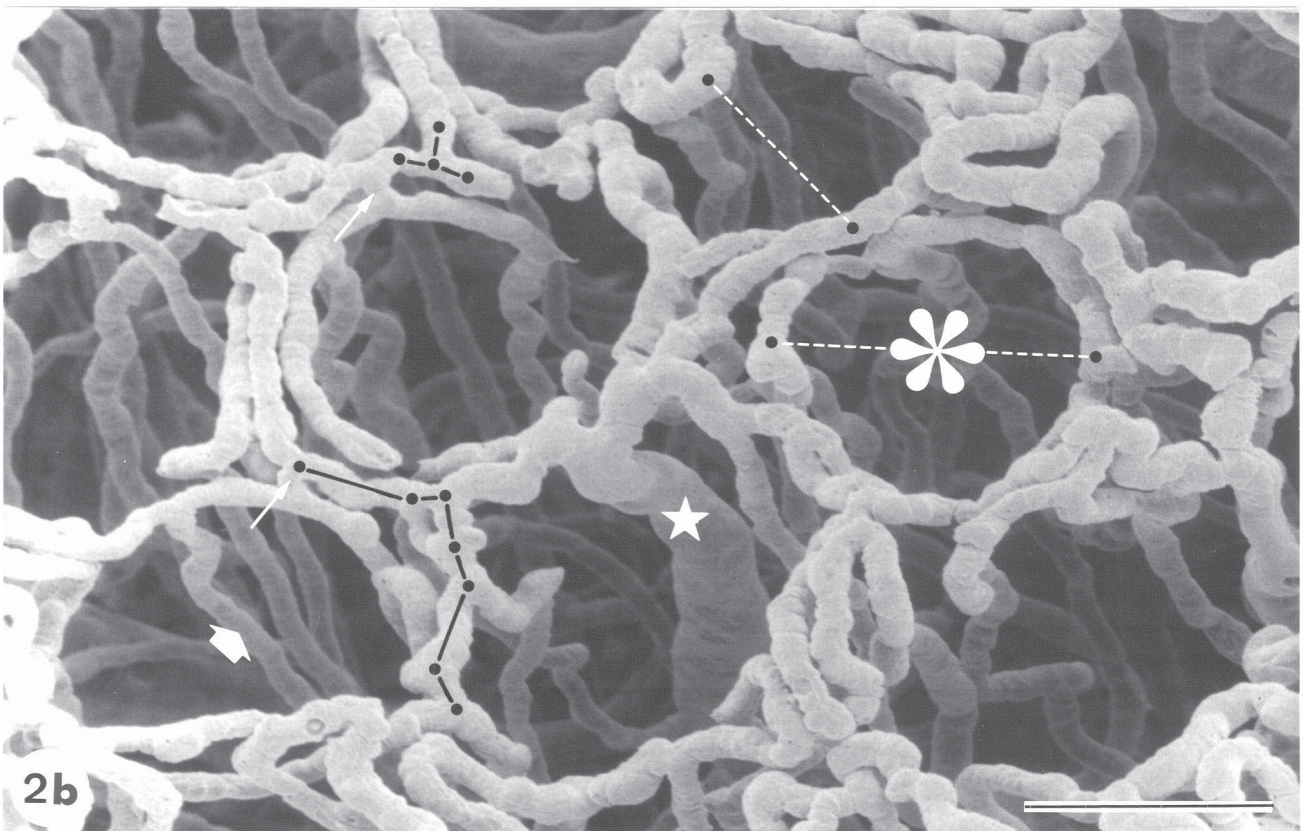
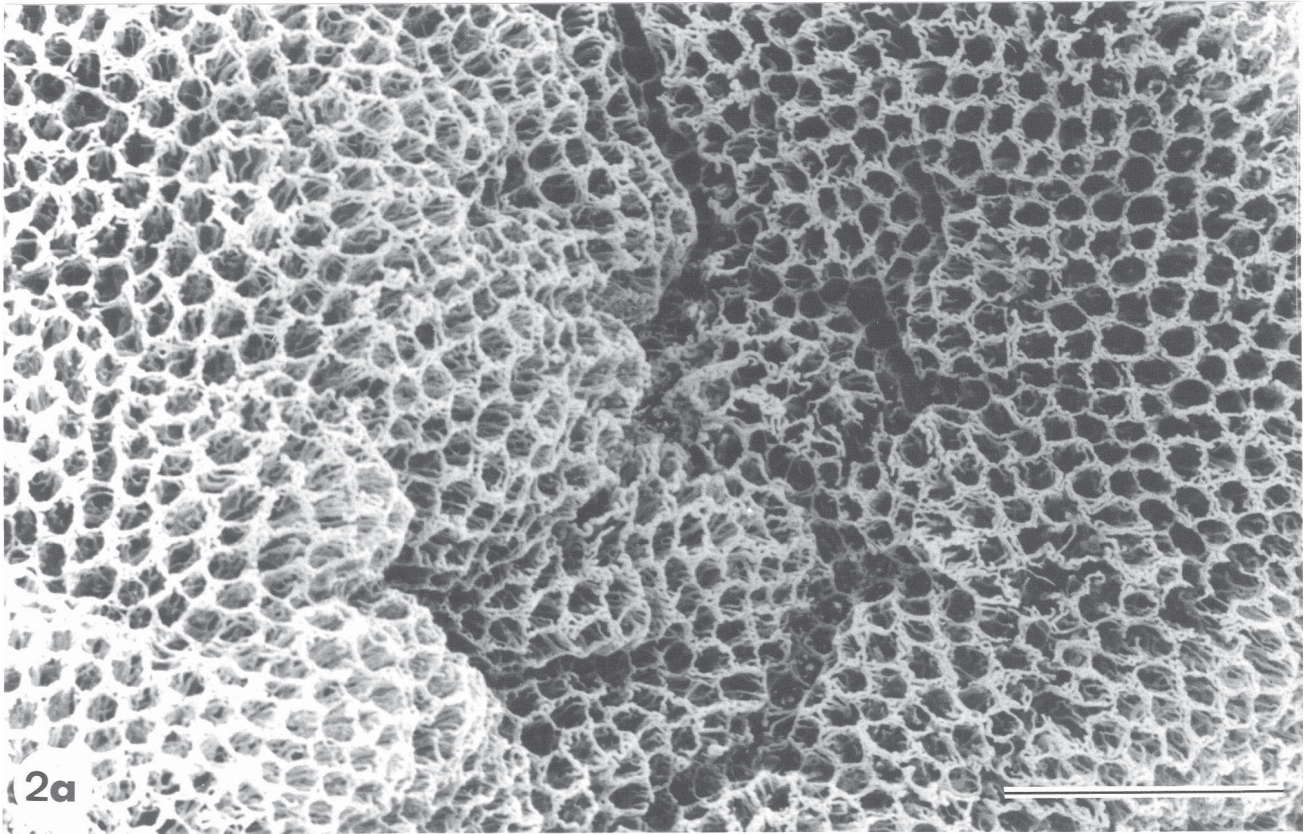
## Results

### Vascular architecture

All specimens showed a complete or nearly complete filling of the vascular system. The microvascular corrosion casts of all investigated segments of the large intestine revealed similar structures and vascular architecture to those previously described by Aharinejad *et al.* (1991) and Skinner *et al.* (1995). The mucosal capillary plexus is supplied by arteries that divide within the submucosa to subepithelial capillaries (Fig. 1a). The mucosal capillary network is drained by venules originating immediately under the mucosal surface and pass to submucosal veins (Figs. 1a,b). The mucosal capillary network is arranged in a honeycomb pattern around the mucosal glands (Figs. 2a,b). All



Microvascular patterns of the human large intestine



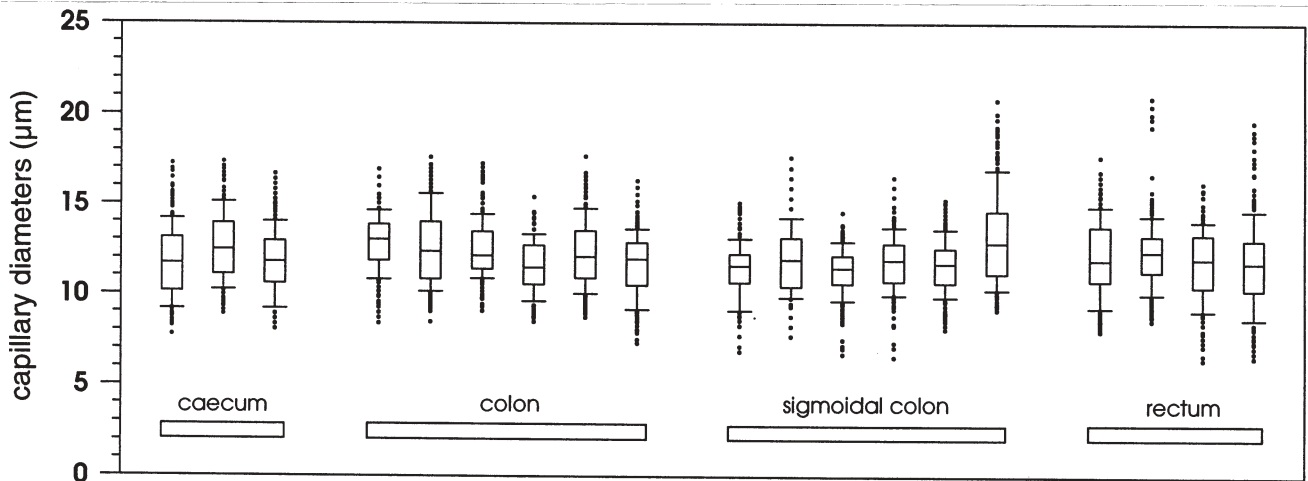


**Figure 3.** Diameters of the measured capillaries. In each specimen, the diameters of at least 50 vessels were determined at five randomly chosen points between two branching points. The mean of all vessel diameters is  $12.04 \pm 1.9 \mu\text{m}$ . Note the comparatively low, statistically not significantly different, variance in the individual segments of the large intestine. Box plot with lower boundary indicating the 25th percentile, upper boundary the 75th percentile. Error bars indicate the 10th and 90th percentile. In addition, all outlying values are graphed.

measurements were performed on capillaries of the mucosa, which were identified as capillaries by their localisation, diameter and the criteria given by Hodde and Nowell (1980) or Nowell and Lohse (1974) (Figs. 2a,b). The measurements were made in the plane of the mucosal surface and across the hexagonal capillary meshes. Arterial and venous vessels of the submucosa and of the deeper layers were not considered. The average luminal diameter of the measured capillaries was  $12.04 \pm 1.9 \mu\text{m}$ ; the minimal diameter was  $6.4 \mu\text{m}$ , while the maximal diameter was  $20.9 \mu\text{m}$  (Fig. 3).

#### Intercapillary distance

Comparison of the individual intercapillary distances within the given segment of the large intestine did not reveal significant inter-individual differences (Figs. 4a-4d). Because there were no significant differences between the individual segments when compared by Mann-Whitney rank sum test, the groups were combined (Fig. 5a). The average intercapillary distances were  $98.09 \pm 22.8 \mu\text{m}$  for the caecum,  $102.0 \pm 22.6 \mu\text{m}$  for the colon,  $101.9 \pm 23.9 \mu\text{m}$  for the sigmoidal colon and  $107.8 \pm 23.6 \mu\text{m}$  for the rectum. For review of the averaged intercapillary distances of the different segments of the large intestine as well as the minima and maxima and the numbers of measured distances, see Table 2.

#### Interbranching distance

Statistical testing of individual interbranching distances within the given segment of the large intestine proved no significant differences (Figs. 6a-6d). Furthermore, no

statistic differences were found in the group comparison (Fig. 5b). The average interbranching distances were  $46.2 \pm 27.8 \mu\text{m}$  for the caecum,  $50.5 \pm 26.2 \mu\text{m}$  for the colon,  $50.6 \pm 26.5 \mu\text{m}$  for the sigmoidal colon and  $56.1 \pm 33.6 \mu\text{m}$  for the rectum.

#### Branching angle

Comparison of the individual branching angles of the capillaries within a given segment of the large intestine did not reveal significant inter-individual differences (Figs. 7a-7d). Thus, the group comparison of all segments did not, again, show any significant differences (Fig. 5c). The average branching angle of the caecum is  $86.8 \pm 29.6^\circ$ , of the colon  $87.9 \pm 26.6^\circ$ , of the sigmoidal colon  $87.8 \pm 29.4^\circ$  and of the rectum  $89.1 \pm 27.5^\circ$ . The average branching angles of the different large intestine segments and the number of measurements are listed in Table 2. The statistics revealed on all segments of the large intestine that there are no intersegmental differences.

#### Discussion

The aim of this study was to perform quantitative morphometry of the microvascular unit in different segments of the large intestine by means of microvascular corrosion casts. The investigation was carried out on human surgical specimens. A satisfactory filling was achieved in all specimens. Leakage of the resin was not observed and endothelial cell nucleus imprints were detectable on all casts. Thus, the quality of the casts of surgical material was



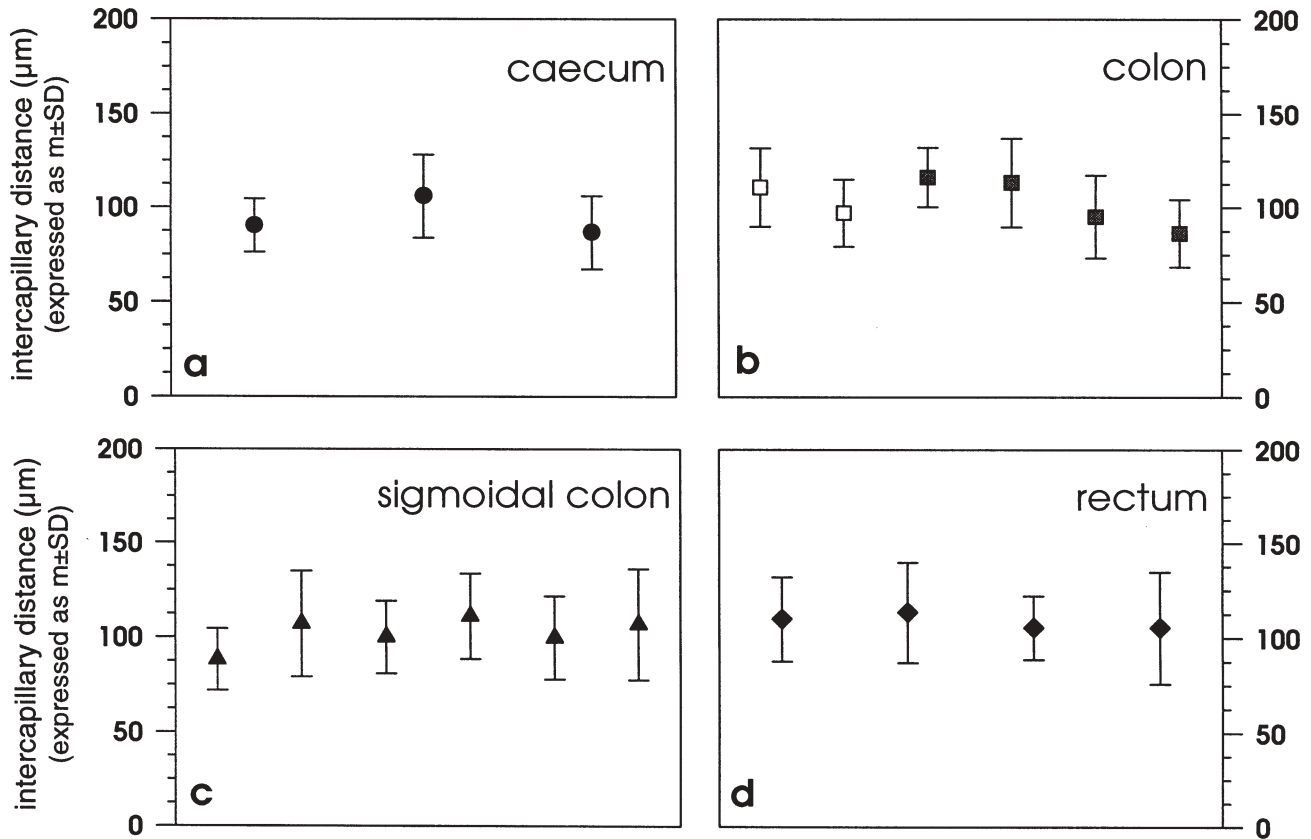


**Figure 4.** Intercapillary distances of different segments of the large intestine. (a) = caecum (n = 3), (b) = ascending (n = 2; open box) and descending colon (n = 4; shaded box), (c) = sigmoidal colon (n = 6) and (d) = rectum (n = 4). Comparisons of specimens removed from the same colonic segment demonstrate that the distributions are very similar. Furthermore, the intercapillary distances within the colon (b) were homogeneously distributed irrespective of their origin from the ascending or descending colon. The differences were not statistically significant. The intercapillary distances are expressed as the mean plus/minus the standard deviation ( $m \pm SD$ ).

comparable to that of casts obtained from experimental animals under controlled conditions (Konerding, 1991).

The architecture of the capillary network in all large intestine segments studied is consistent with the qualitative descriptions of Aharinejad *et al.* (1991, 1992), Browning and Gannon (1986) and Skinner *et al.* (1995). Compared to the stomach, the microvascular pattern of the colon shows numerous similarities (Browning and Gannon, 1986). However, comparisons with the microvascular architecture of the small intestine reveal some differences. Spanner (1932) presented different types of microvascular architecture within individual villi. He discerned a fountain-like arrangement, in which the arteriole reaches the top of the villus without branching ("fountain-type") from a deeply interconnected type ("step ladder") and a "tuft-type." This classification, also supported by Aharinejad *et al.* (1991)

and Browning and Gannon (1986), cannot be made in the colon. However, it should be kept in mind that such an arrangement is most unlikely in the colon because of the missing villi.

Browning and Gannon (1986) described a gradual reduction of both mucosal capillary density and average meshwork width towards the more distal colon. Aharinejad *et al.* (1991) discussed this as a reflection of the decreased reabsorption of water in the distal colon. These findings are inconsistent with our data, since we found in all segments of the colon similar intercapillary distances. Possibly this discrepancy can be explained in terms of species specificity based on different functions and nutrition. The human colon is comparatively much shorter than in the rodents. Additionally, it should be kept in mind

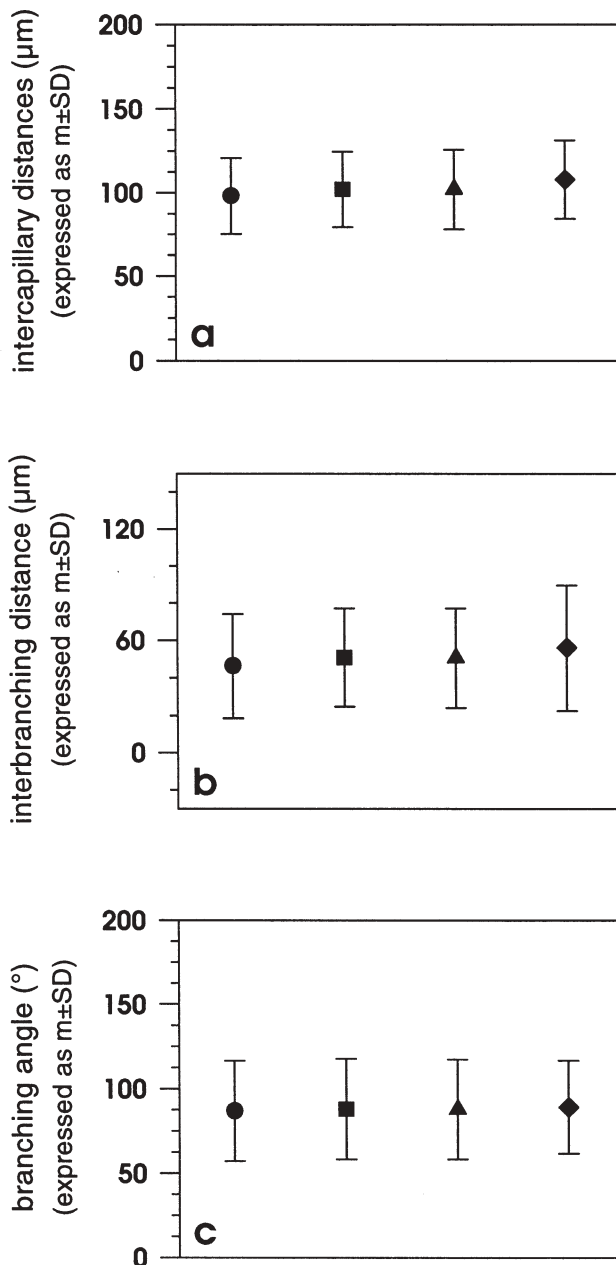


**Figure 5.** Intercapillary distances (a), interbranching distances (b) and branching angles (c) of different segments of the large intestine. Group comparisons within all segments reveal no statistic differences. The intercapillary distances and the interbranching distances as well as the branching angles are expressed as mean  $\pm$  standard deviation ( $m \pm SD$ ). Caecum = circles, colon = squares, sigmoidal colon = triangles, rectum = diamonds.

that the above mentioned papers are basically descriptive ones.

On the other hand side, one should not forget that there must not necessarily be a direct correlation between the vascular density (or intercapillary distance) and the resorptive function. Other parameters such as an increased number of fenestrae can enhance the resorptive function, too. Furthermore, differences in the depth of the mucosal glands of the individual colonic segments might be paralleled by differences in the depth of the mucosal vascular plexus and, thus, cause a higher total vascular volume with higher resorption.

Araki *et al.* (1996) approached this question by counting the layers of the mucosal capillary loops in human ascending colons and sigmoid colons. They described the capillary plexus in the ascending colon as a multilayered plexus and that of the sigmoid colon as almost single-layered. This is not in line with our observations. We found even in the rectum in 3 out of 4 specimens more than a single layered plexus. In two rectum specimens we saw three or more capillary layers per capillary loop. This heterogeneity of the number of capillary layers was seen in all colonic segments of the colon as well as in the individual specimens. Since Araki *et al.* (1996) did not give any information on the number of examined areas per surgical specimen and the intra-individual variances of the capillary layers, we can not explain this discrepancy.

#### Acknowledgements

This study was supported by a grant of the European Community (Human Capital and Mobility Programme ERB CHRX-CT9-0593: Mechanisms for the Regulation of Angiogenesis). The image analyzing system used for this study was granted by the Robert Müller-Stiftung Mainz für Herz-Kreislauf-Forschung (Robert Müller-Foundation for Cardiovascular Research).

The authors would like to thank Mrs. K. Bahr, A. de Cuvry, Ch. Peigney and D. Volland for technical assistance.

#### References

- Aharinejad S, Lametschwandtner A, Franz P, Firbas W (1991) The vascularization of the digestive tract studied by scanning electron microscopy with special emphasis on the teeth, esophagus, stomach, small and large intestine, pancreas and liver. *Scanning Microsc.* **5**, 811-849.
- Aharinejad S, Gangler P, Hagen D, Firbas W (1992) Studies on the microvascularization of the digestive tract by scanning electron microscopy of vascular corrosion casts. 1. Large intestine in rats and guinea pigs. *Acta Anat.* **144**, 278-283.
- Araki K, Furuya Y, Kobayashi M, Matsuura K, Ogata T, Isozaki H (1996) Comparison of the mucosal microvasculature between the proximal and distal human



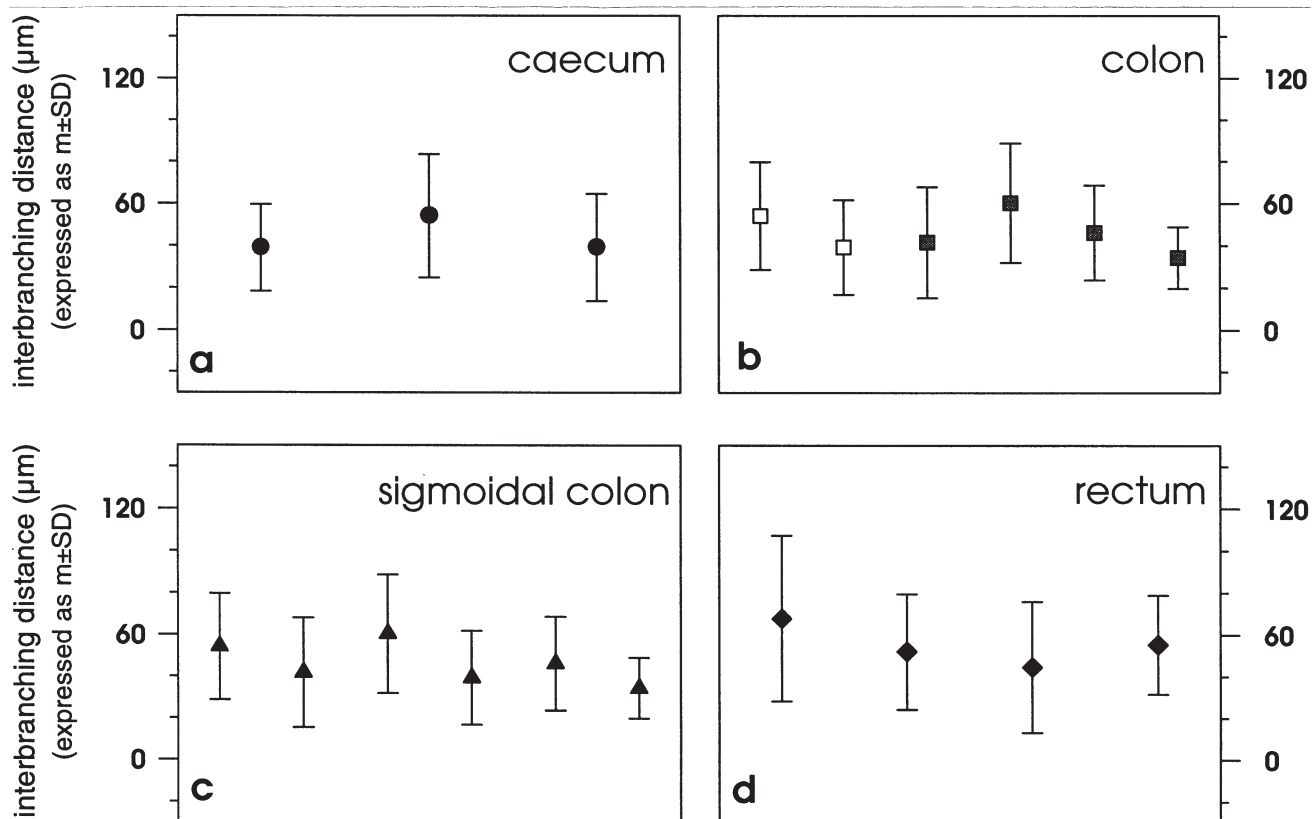


**Figure 6.** Interbranching distances of different segments of the large intestine. (a) = caecum (n = 3), (b) = ascending (n = 2; open box) and descending (n = 4; shaded box) colon, (c) = sigmoidal colon (n = 6) and (d) = rectum (n = 4). Group comparisons show that there are no significant differences. Furthermore, the interbranching distances within the colon (b) were homogeneously distributed irrespective of their origin from the ascending or descending colon. By means of statistic comparison no significant differences were found. The interbranching distances are expressed as mean  $\pm$  standard deviation (m  $\pm$  SD).

colon. *J. Electron Microsc.* **45**, 202-206.

Boyde A (1973) Quantitative photogrammetric analysis and qualitative stereoscopic analysis of SEM images. *J. Microsc.* **98**, 452-471.

Boyde A (1974) Photogrammetry of stereopair SEM images using separate measurements from two images. *Scanning Electron Microsc.* **1974**, 101-108.

Browning J, Gannon B (1986) Mucosal microvascular organization of the rat colon. *Acta Anat.* **126**, 73-77.

Christofferson RH, Nilsson BO (1990) Microvascular corrosion casting with analysis in the scanning microscope. *Scanning* **10**, 43-63.

Darien BJ, Sims PA, Stone WC, Schilly DR, Dubielzig RR, Albrecht RM (1993) Ischemia/reperfusion injury of the ascending colon in ponies: A correlative study utilizing microvascular histopathology and corrosion casting. *Scanning Microsc.* **7**, 1311-1320.

Dart AJ, Synder JR, Harmon FA (1992) Microvascular circulation of the descending colon in horses. *Am. J. Vet. Res.* **53**, 1001-1006.

Hodde KC, Nowell JA (1980) SEM of microcorrosion casts. *Scanning Electron Microsc.* **1980**, II, 89-106.

Konerding MA (1991) Scanning electron microscopy of corrosion casting in medicine. *Scanning Microsc.* **5**, 851-865.

Konerding MA, Miodonski AJ, Lametschwandtner A (1995) Microvascular corrosion casting in the study of tumor vascularity: A review. *Scanning Microsc.* **9**, 1233-1244.

Lametschwandtner A, Miodonski A, Simonsberger P (1980) On the prevention of specimen charging in scanning electron microscopy of vascular corrosion casts by attaching conductive bridges. *Mikroskopie* **36**, 270-273.

Lametschwandtner A, Lametschwandtner U, Weiger T (1984) Scanning electron microscopy of vascular corrosion

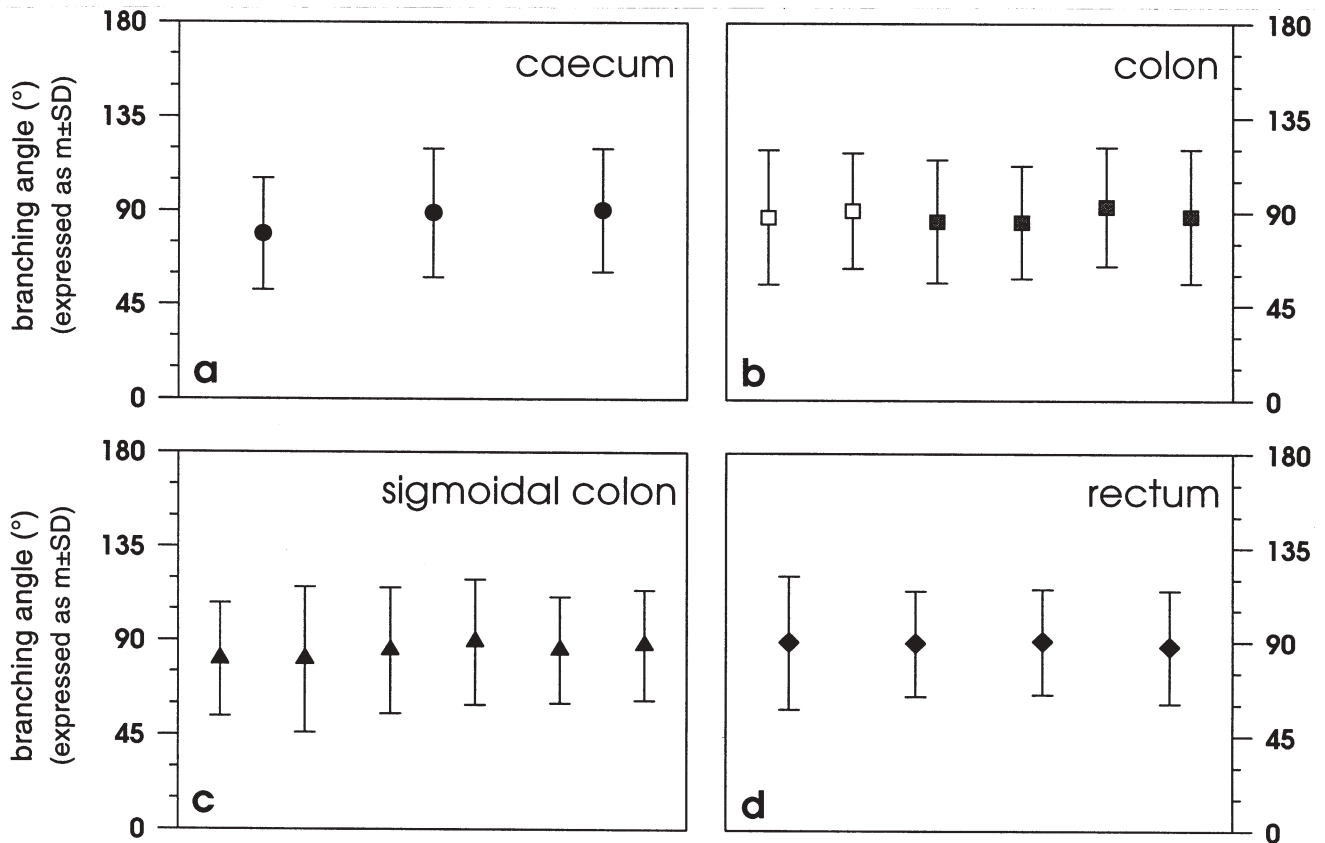


**Figure 7.** Branching angles of different segments of the large intestine. (a) = caecum (n = 3), (b) = ascending (n = 2; open box) and descending (n = 4; shaded box) colon, (c) = sigmoidal colon (n = 6) and (d) = rectum (n = 4). Statistic comparison indicates no significant differences. The interbranching angles are expressed as mean  $\pm$  standard deviation ( $m \pm SD$ ).

casts - technique and applications: Updated review. *Scanning Microsc.* **2**, 663-695.

Lametschwandtner A, Lametschwandtner U, Weiger T (1990) Scanning electron microscopy of vascular corrosion casts - technique and applications: Updated review. *Scanning Microsc.* **4**, 889-941.

Malkusch W, Konerding MA, Klapthor B, Bruch J (1995) A simple and accurate method for 3-D measurements in microcorrosion casts illustrated with tumor vascularization. *Ann. Cell. Path.* **9**, 69-81.

Nowell JA, Lohse CL (1974) Injection replication of the microvascular for SEM. *Scanning Electron Microsc.* **1974**, 267-274.

Skinner SA, Tutton PJM, O'Brien PE (1990) Microvascular architecture of experimental colon tumors in the rat. *Cancer Res.* **50**, 2411-2417.

Skinner SA, Frydman GM, O'Brien PE (1995) Microvascular structure of benign and malignant tumors of the colon in humans. *Digestive Dis. Sci.* **40**, 373-384.

Spanner R (1932) Neue Befunde über die Blutwege

der Darmwand und ihre funktionelle Bedeutung (New results on blood vessels of the small intestine and their functional importance). *Morph. Jahrb.* **69**, 394-454.

### Discussion with Reviewers

**A. Lametschwandtner:** In your introductory remarks you clearly state that the microcirculatory unit is defined by intercapillary distances, interbranching distances, and branching angles. In order to analyze microvascular units in different species and organs, a matter of particular interest for studies on the evolutionary constraints of the microvascular unit, it would be quite interesting to know up to which diameters of arterial and venous vessels the measurements were done. Could you please give the luminal diameters of the largest vessels where the three parameters were measured?

**Authors:** As shown in Figure 3, we have assessed the above mentioned parameters only on capillaries of the mucosal plexus, not on arteries and veins. The tenth

percentile was 9.7  $\mu\text{m}$ , the ninetieth percentile was 14.4  $\mu\text{m}$ . For comparative evolutionary studies of the microvascular unit, however, it seems to be necessary to take into account additional parameters such as the number, diameter and branching pattern of the supplying arterioles and draining venules since the parameters examined in this study describe only the capillary network.

**A. Ohtsuka:** Are there any segmental differences in the depth of the mucosal glandular vascular plexus; i.e., the distances from the bottoms to the orifices of the crypts? Did you consider the volume of the mucosal gland in each segment?

**Authors:** Since we studied only the mucosal vascular plexus as seen from the luminal aspect, we cannot give information on the total vascular volume of the individual colon segments. For considering the volume of the mucosal glands, we would have needed, additionally, exactly vertically orientated sections of the native or unmacerated tissue.

**S. Patan:** Are the values measured in the present study different from those obtained in the pathological state, as in tumor angiogenesis or chronic diseases of the colon?

**Authors:** From our experience with the microvasculature in xenografted tumors as compared to normal tissues, we expect numerous differences of the measured parameters in human tumors. Until now, however, we have not yet studied enough human primary tumors to give a conclusive, statistically proven answer.

**S. Patan:** Does the observed homogeneity of the measured parameters throughout the colon correspond to the physiological state or is it related to the fact that the observed specimen were derived from surgically resected tumors and might subsequently reflect a vasculature that has been uniformly transformed during tumor angiogenesis?

**Authors:** Our specimens were taken out in a distance of at least 10 cm away from the pathological tissue (tumor, adenoma, or chronic inflammation). A transformation of microvasculature induced by a paracrine release of angiogenic substances is, therefore, most unlikely.

**S. Patan:** Do other honeycomb-like microvascular networks (as in the stomach or around the ovarian follicles) possess a similar pattern concerning the measured parameters?

**Authors:** This is the first 3D-quantitative study of these parameters in microvascular corrosion casts. Thus, we cannot (yet) answer your question.

**S. Patan:** Could the intercapillary distance as related to the number of branching points be a nice measure for the vascular density and subsequently reflect another important characteristic of a vascular network?

**Authors:** No. A quotient of intercapillary distance and number of branching points is void of a dimension and not suitable for measuring the vascular density. For example, if the intercapillary distance was 100  $\mu\text{m}$ , and the interbranching distance 100  $\mu\text{m}$ , your proposed quotient would have the same value as in an area with intercapillary distances and interbranching distances of 10  $\mu\text{m}$ .